# Erosion of Metals by Solid Particle Impingement

by

Richard Arnold Jarrett

Submitted in Partial Fulfillment

of the Requirements for the

Degree of Bachelor of Science

at the

MASSACHUSETTS INSTITUTE OF TECHNOLOGY

May, 1971

Signature of Author .....
Department of Mechanical Engineering, May 24, 1971

Certified by .....
Thesis Supervisor

Accepted by .....
Chairman, Departmental Committee of Theses

Table of Contents

Abstract

The effects of single particle 90° impingement were investigated using a rotating arm erosion tester. The resultant impacts were studied using a scanning electron microscope. The primary mechanism of the this erosion appears to be pure shear. Secondary damage caused by fragments of the specimens and the test apparatus clouds the results of rotating arm erosion tests.

## Introduction

Gradual wear process is commonly known as erosion. The subject of this thesis is erosion caused by solid particle impingement. In many cases, this wear is highly undesirable. Several examples of the detrimental effects of erosion are the following:

1.) The compressor blades of gas turbines when operated over dusty terrains are seriously damaged by erosion. The efficiency of the compressor drops radically as the airfoil surfaces of the blades wear. On small gas turbines the trailing edge of the blades, often as thin as five thousandths of an inch, is consequently readily worn away. In some cases, the life of such turbines is reduced to 10% of its expected life.[1,2] Steam turbines operating in the wet-steam regions are also affected similarly by erosion caused by the water droplets.

2.) In industrial processes involving pipelines such as the catalytic cracking of oil,[3] foreign particles suspended in the fluid can cause serious erosion. This problem is greatest at bends in the lines or at constrictions such as valves where particles are more likely to strike the surfaces.

3.) Erosion due to rain can cause considerable damage to the nose of aircraft. In a radome, not only is the structure of the dome weakened but the effectiveness of the radar is also greatly reduced.[4]

4.) Rocket nozzles can be severely damaged by solid particles carried by the hot gases that flow through them.[5]

On the other hand, erosion can be used beneficially to machine surfaces as in sand blasting or the erosive drilling of hard materials.[6]

Although many people have solved specialized erosion problems when undertaking a specific design task, few until recently have attempted to examine the overall mechanism of erosion. In 1958, Finnie[7] derived equations based on cutting tool theory, for the weight loss of material caused by a particle moving in a known manner. In a later study in 1960, Finnie[8] suggested that two factors were involved in the amount of material eroded. These were the conditions of the fluid flow and the mechanism of material removal. For ductile materials, he predicted the manner in which material removal varies with particle direction and speed. Although his figures did not disagree with the results of metal cutting tests, they could not accurately determine the amount of erosion that occurred.

For brittle materials, Bitter predicted the initial fracture of the material by calculating stresses between the particle and the surface.[3] In practice, a distinction between brittle and ductile behavior is very difficult to determine. Nominally brittle materials may act in a ductile fashion when small loads are applied.[9] Since none of the proposed theories

seem to predict the amount of erosion accurately, some researchers have proposed that the erosion strength of a material is an entirely separate property unrelated or only slightly related to the known material properties.[10]

The results of previous investigators can be most easily summarized by considering four main variables: angle of impingement, particle size, speed, and material properties. General agreement in the literature exists regarding the effect of the angle of particle impingement. This effect is presented in Figure 1 for ductile-acting materials and in Figure 2 for brittle-acting materials.

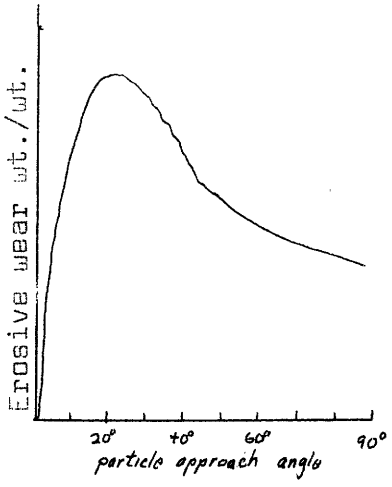


Fig. 1 Erosive wear of ductile materials

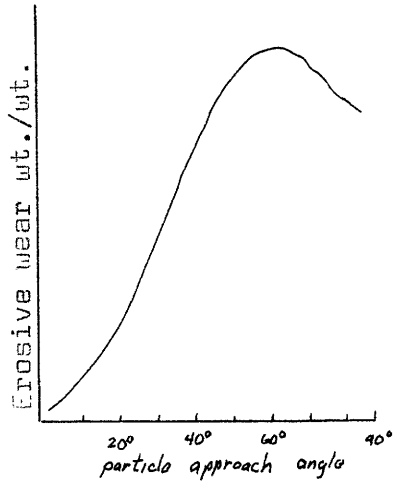


Fig. 2 Erosive wear of brittle materials

It is interesting to note that the same material may act either in a brittle or ductile manner depending on the size of the impinging particle. It has been generally found that erosion increases with increasing particle size up to a critical size. Agreement as to the exact relation between erosion and particle

size has not been reached; both linear and non-linear functions have been reported.

The amount of erosion has been shown to increase with increasing velocity. For ductile materials, erosion has been shown to be proportional to about the 2.3 power of the velocity. Erosion in brittle materials also rises as a power of the velocity, but this power varies from 1.4 to 5.1 depending on the specific material. Other factors which can affect the amount of erosion but which are unrelated to its actual mechanism are particle composition and concentration of erosive particles in a fluid.

Most previous studies have dealt with the weight loss of material per weight of impacting particles. This study is primarily concerned with the effect of single particle impingement. By studying the effect under magnification, it may be possible to determine the mechanisms of material failure. A relation between failure and grain size is also investigated.

## Experimental Procedure

The method employed to achieve a single particle impingement consists of dropping a silicon carbide particle into the path of a specimen moving at a known velocity and impact angle. This control of the specimen is attained by placing it on a rotating arm. To eliminate aerodynamic effects the whole experiment is performed in a vacuum.

Test Apparatus:

A rotating arm erosion tester had been designed and built in the Materials Processing Laboratory. This apparatus consisted of a twelve inch arm which rotated in a vacuum chamber, an air turbine to drive the arm, and a photo transistor coupled with an electronic counter to measure the speed of the arm. In order to obtain a low vacuum for accurate determination of impingement speeds, silicon rubber gaskets and neopreme "O" rings were used on shafts and demountable surfaces. A mercury manometer was used to measure the vacuum. An arm was designed and built to undergo constant stress throughout its length and to withstand the bending moment created by the specimens. The apparatus is shown in Figures 3 through 9.

Test Procedure:

Tests were performed on the following three materials:

a.) 1020 C.R. steel

both as received and annealed for 1 hour @ 1728°F

annealed specimen grain size 35 $\mu$

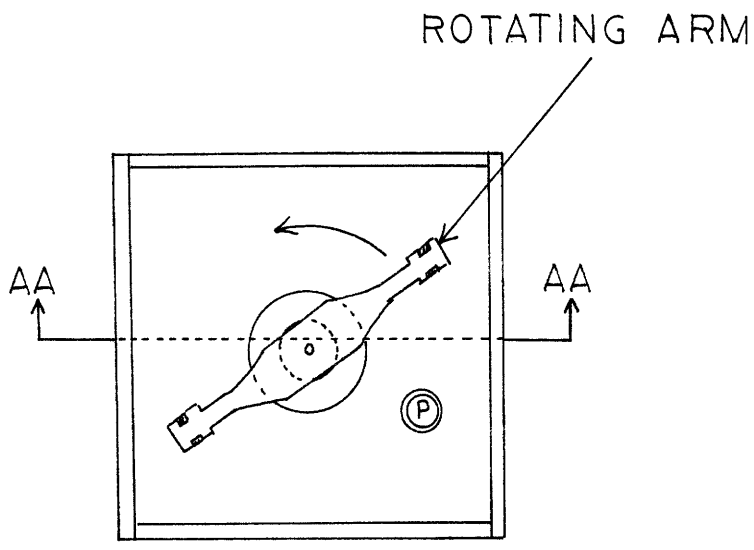


— TOP VIEW: COVER REMOVED —

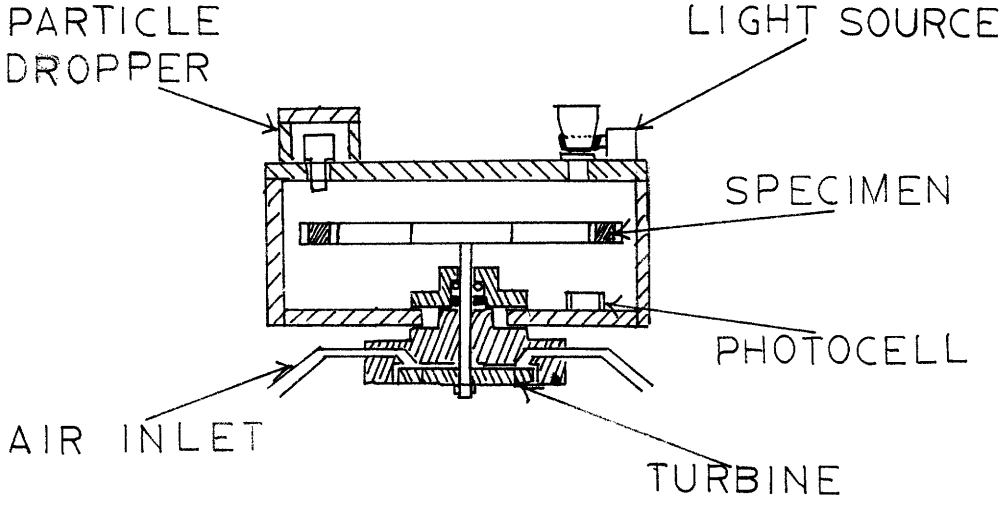


— SECTION AA —

FIG. 3 TEST CHAMBER

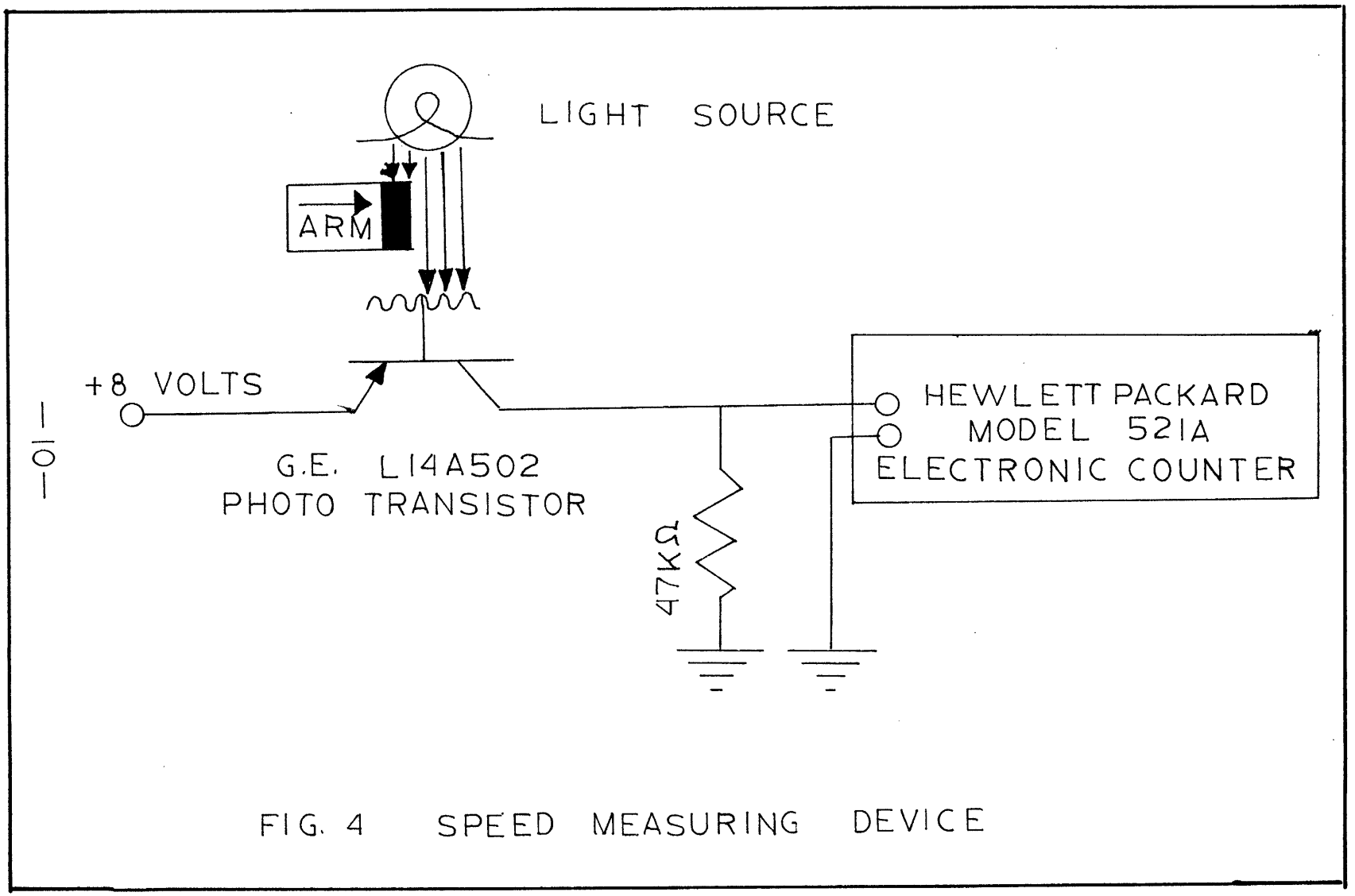


FIG. 4 SPEED MEASURING DEVICE

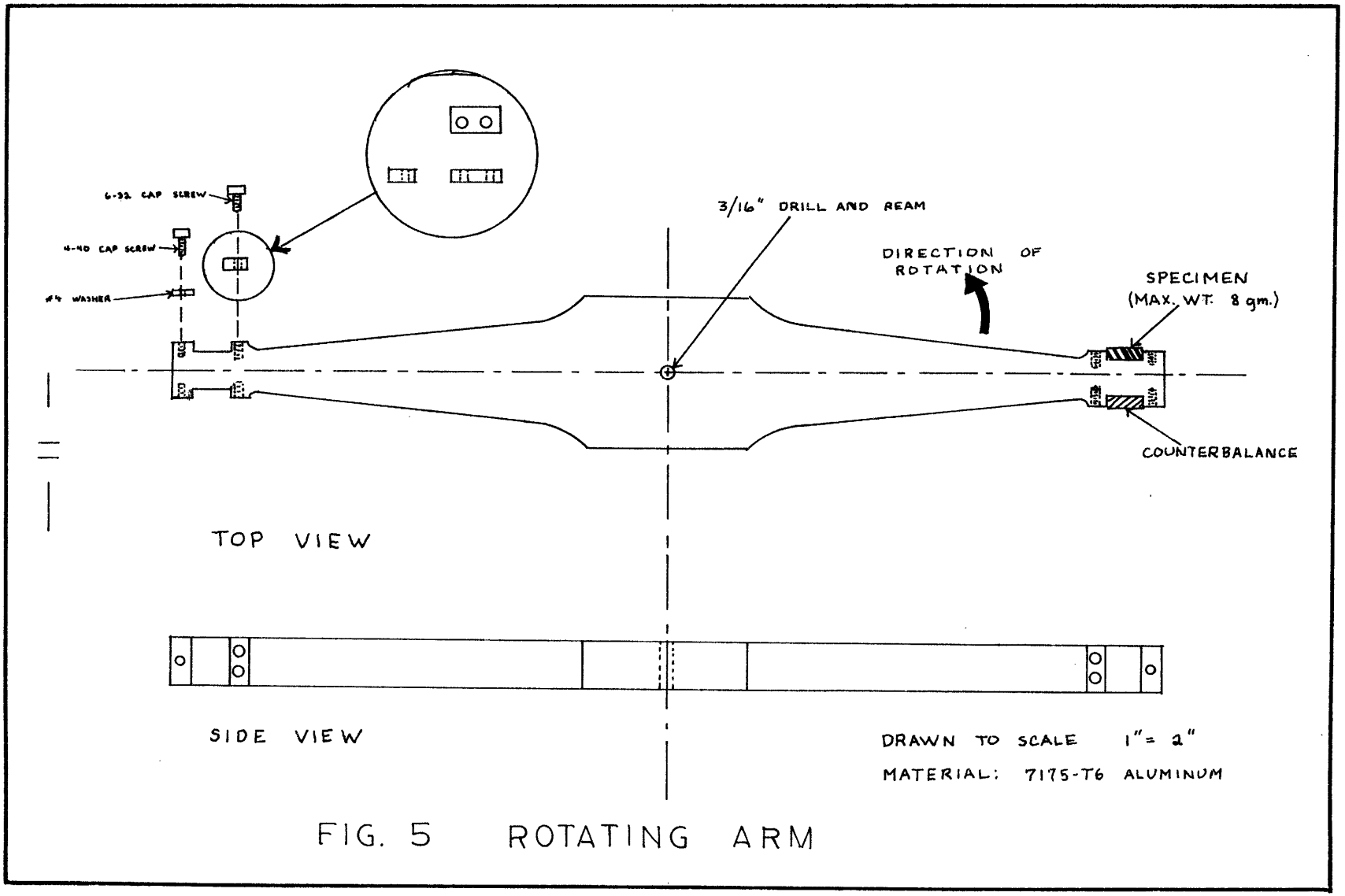


FIG. 5 ROTATING ARM

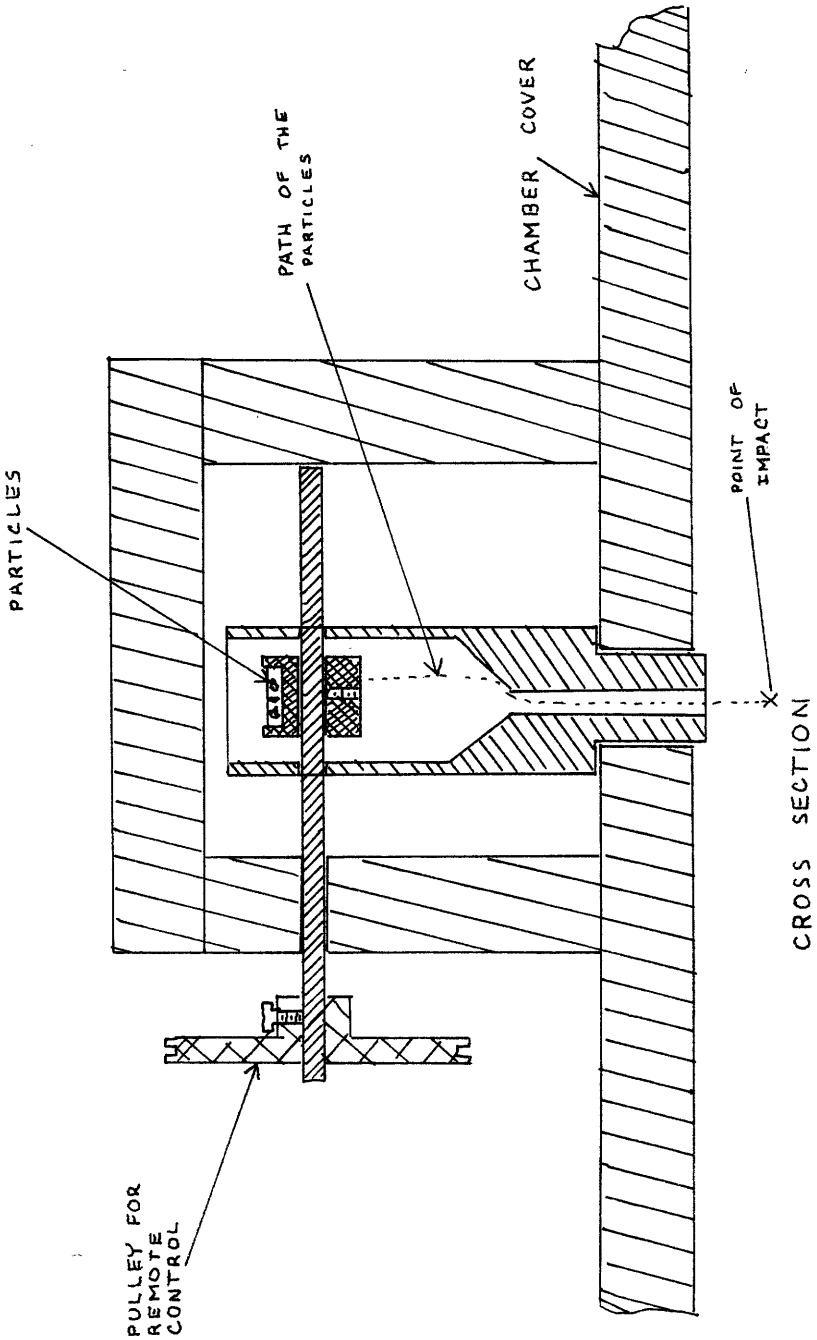


FIG. 6 PARTICLE DROPPER

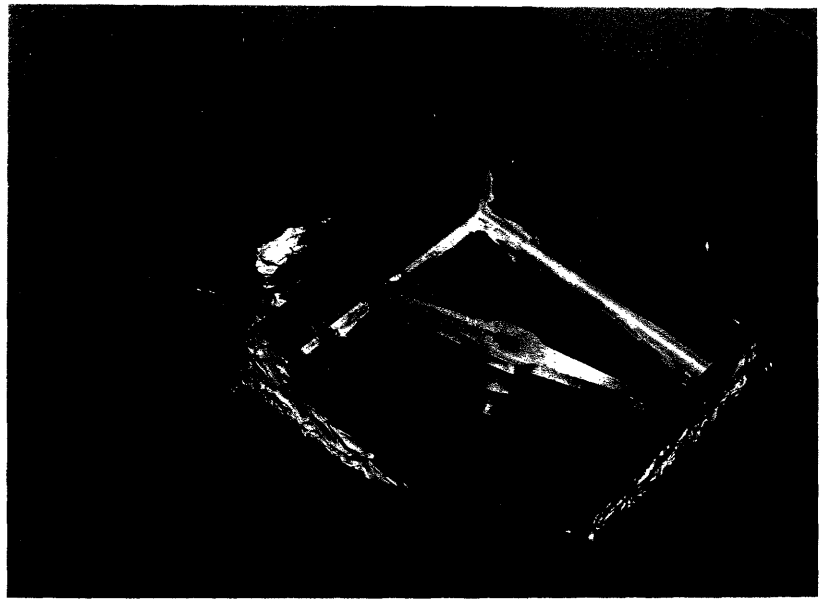

Fig. 7 Vacuum Test Chamber

Fig. 8 Chamber Cover and Particle Dropper

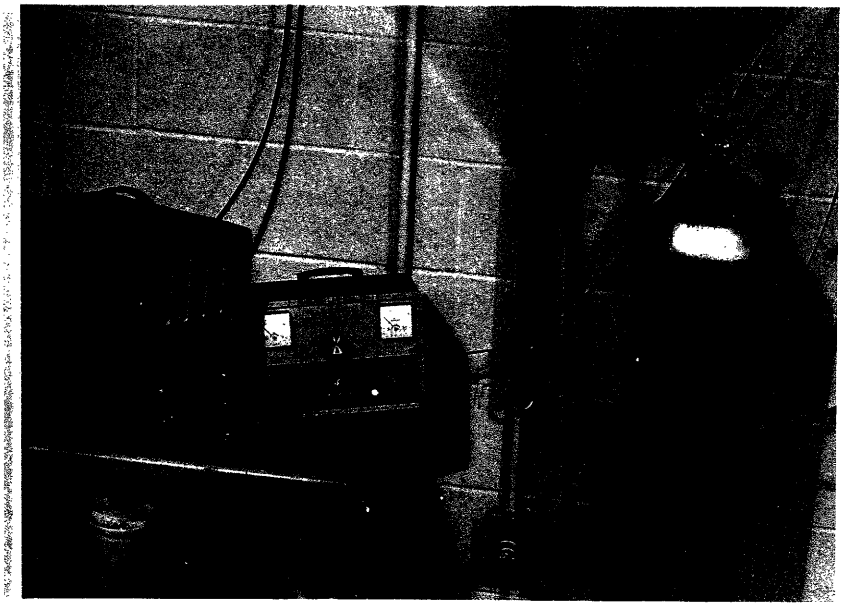

Fig. 9 Control Apparatus

b.) Modified 1010 steel* ($\alpha$ phase ), forged @ 1350°F

both as received and annealed for 1 hour @ 1100°F

annealed specimen grain size 1$\mu$

Composition:

.6% Magnesium
.13% Carbon
.5% Titanium
.17% Plutonium

c.) Doped Titanium alloy*, forged @ 1400°F

both as received and annealed for 1 hour @ 1100°F

annealed specimen grain size 1$\mu$

Composition:

1.5% Hafnium
.5% Zirconium
.15% Chromium
.12% Molybdenum

To prevent corrosion during annealing, the 1010 steel and titanium samples were heated in a vacuum of less than $10^{-4}$ torr. All of the specimens were milled to a uniform size of ½" x ½" x ⅛". They were then polished with successively finer grades of emery and polishing wheels terminating with 4-0 paper for the 1020 steel and 5$\mu$ abrasives for the modified 1010 and titanium alloys. All polishing was done before heat treating to avoid work hardening of the surface.

In the erosion tests, the specimens were mounted on the arm, the silicon carbide particles ( 60 mesh or 250-500$\mu$ ) loaded

*The 1010 steel and titanium samples were obtained from Dr. Ernest Abramson at the U.S. Army Materials Research Center in Watertown, Massachusetts.

into the dropping mechanism, and the cleaned chamber evacuated. For the 1020 steel, a vacuum of 1 mm. was obtained for all the runs except the 1000 ft/sec. run at which the vacuum was 2 mm. For the 1010 steel and titanium alloy, a vacuum of 3 mm. was obtained for all the runs except for the 1000 ft/sec. runs at which the vacuum was 4 mm. The poorer vacuum at high speeds was caused by the deterioration of the "O" ring seal on the shaft. Small leaks developed in the chamber which accounted for the poorer vacuum during the modified steel tests. The vacuum was measured by comparing the manometer reading of the chamber to the barometric pressure. The barometric pressure was determined by connecting the vacuum pump directly to the manometer.

After a specified vacuum had been obtained, the arm was then rotated by accelerating the turbine with compressed air. For the lowest speed ( 100 feet per second ), a steady state speed was attained. For the higher speeds, the arm was run at an approximately constant acceleration. The particles were dropped when the counter indicated the correct speed. In all cases, the total error in the collision speed was not more than 10%. A small enough number of particles was always dropped to insure that only single particle impacts occurred. After the particles were dropped, the apparatus was shut down and the specimens removed. The specimens were then examined and photographed using a JELCO model JSM3- Scanning Electron Microscope. Stereo photographs were taken to permit three dimensional analysis.

## Results

The scanning electron microscope pictures are presented on the following pages.

Fig. 10 CR 1020 Steel, 100 feet/sec.


Fig. 11 Annealed 1020 Steel, 100 feet/sec.

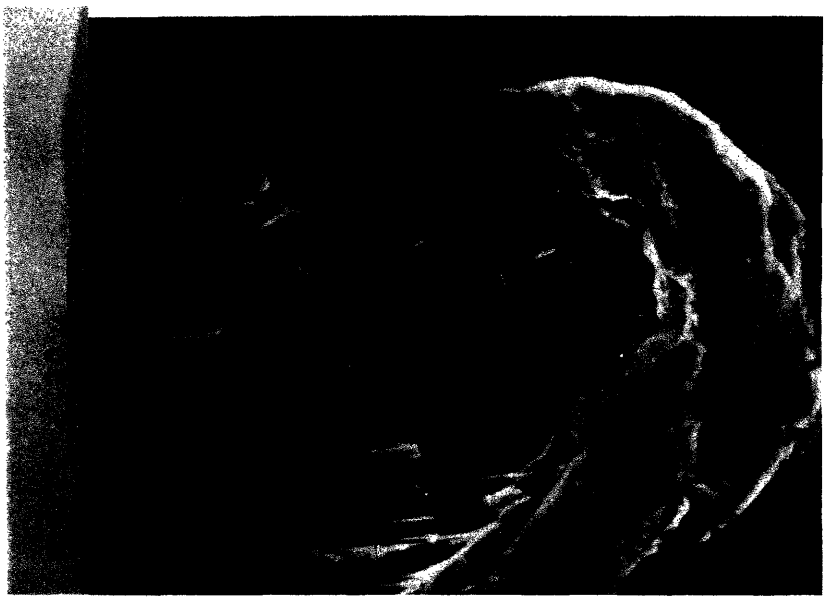

Fig. 12 Annealed Modified 1010 Steel,100 Feet/sec.

Fig. 13 Annealed Modified 1010 Steel, 100 feet/sec.

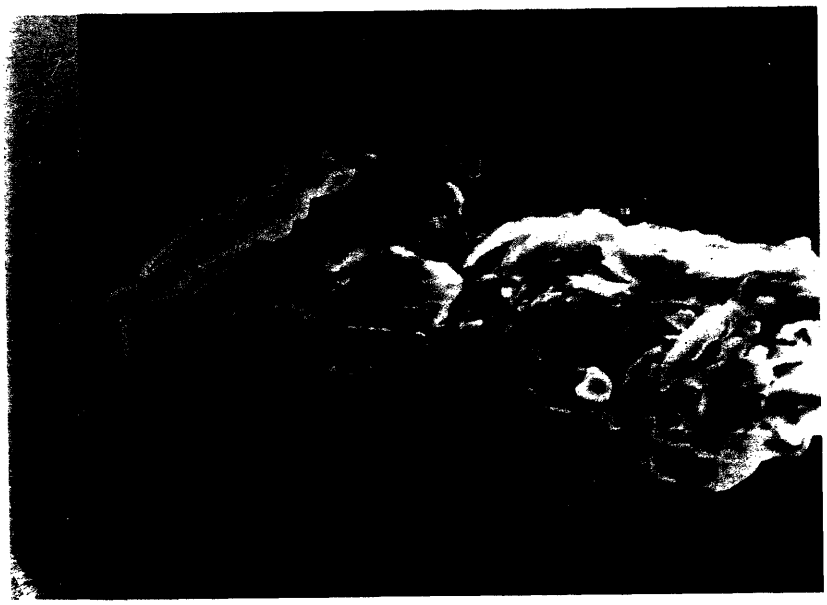

Fig. 14 A.R. Titanium Alloy, 100 feet/sec.

Fig. 15 Annealed Titanium Alloy, 100 feet/sec.


Fig. 16 A.R. Modified 1010 Steel, 300 feet/sec.

Fig. 17 Annealed Modified 1010 Steel, 300 feet/sec.


Fig. 18 A.R. Titanium Alloy, 300 feet/sec.

Fig. 19 Annealed Titanium Alloy, 300 feet/sec.


Fig. 20 CR 1020 Steel, 500 feet/sec.

Fig. 21 Annealed 1020 Steel, 500 feet/sec.

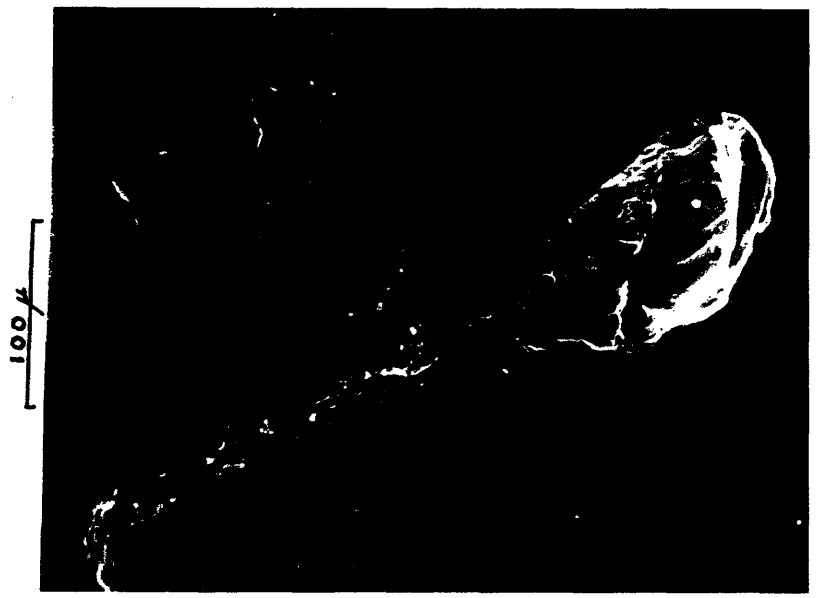


Fig. 22 A.R. Modified 1010 Steel, 500 feet/sec.

Fig. 23 A.R. Modified 1010 Steel, 500 feet/sec.

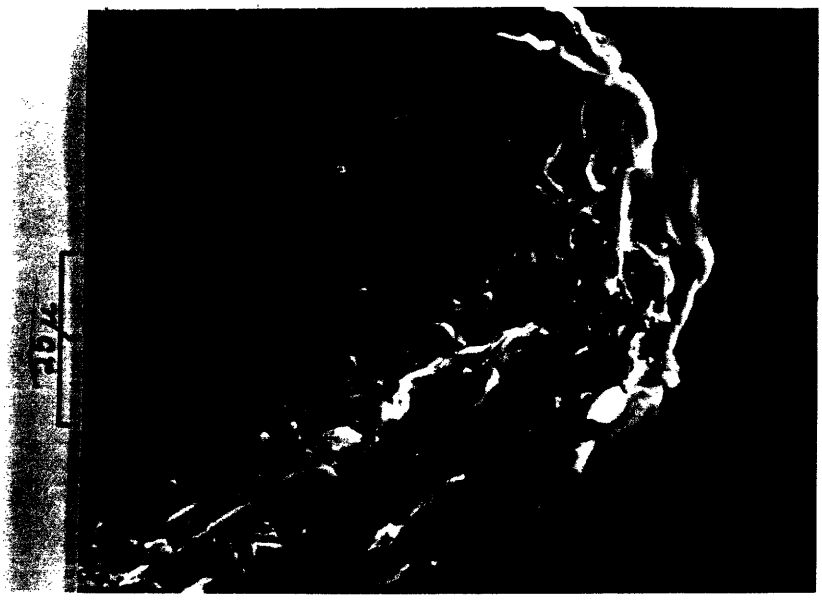

Fig. 24 A.R. Modified 1010 Steel, 500 feet/sec.

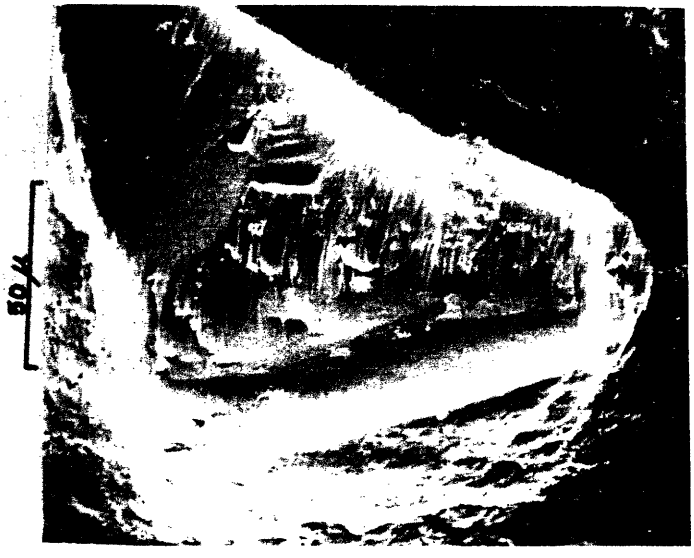

Fig. 25 Annealed Modified 1010 Steel, 500 feet/sec.


Fig. 26 A.R. Titanium Alloy, 500 feet/sec.

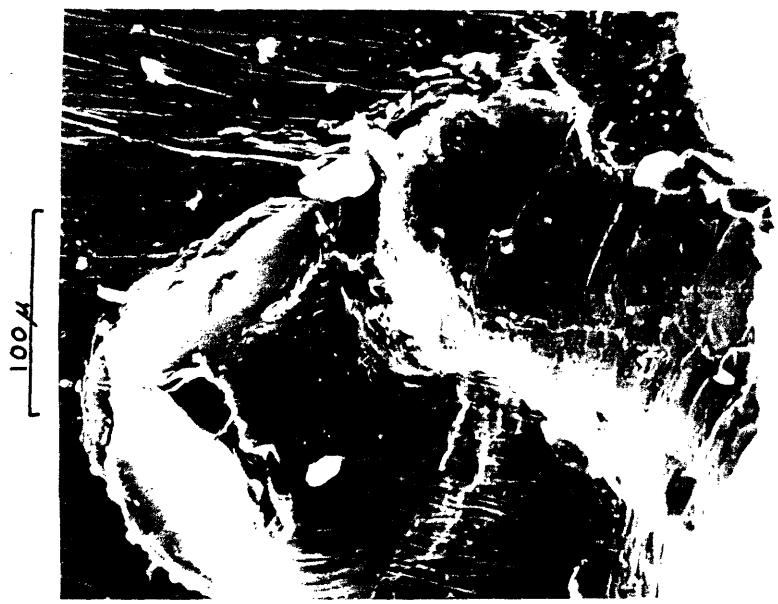


Fig. 27 CR 1020 Steel, 800 feet/sec.

Fig. 28 Annealed 1020 Steel, 600 feet/sec.

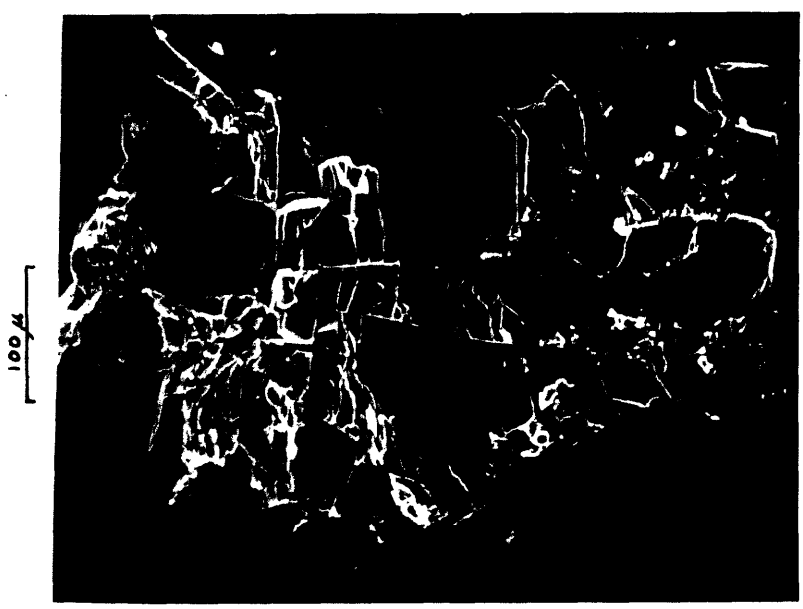


Fig. 29 A.I.S. Modified 1010 Steel, 800 feet/sec.


Fig. 30 A.R. Modified 1010 Steel, 800 feet/sec.

Fig. 31 A.R. Modified 1010 Steel, 800 feet/sec.

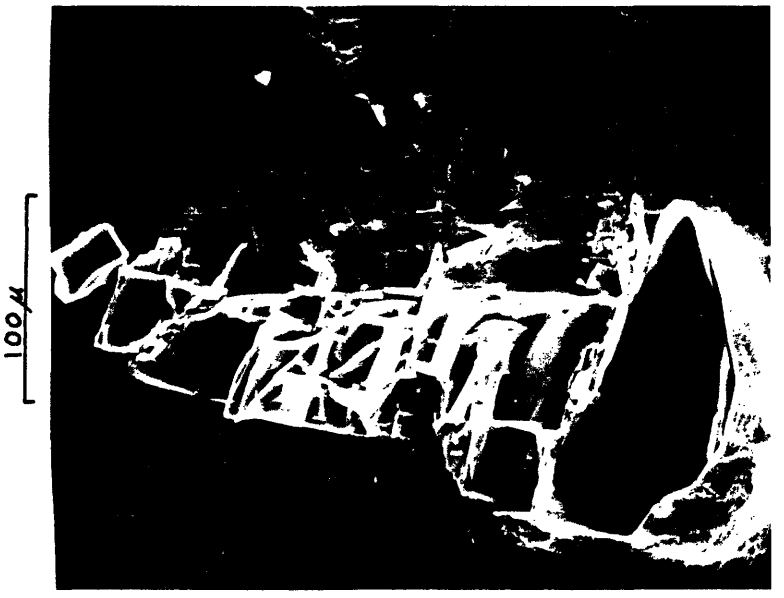


Fig. 32 Annealed Modified 1010 Steel, 800 feet/sec.

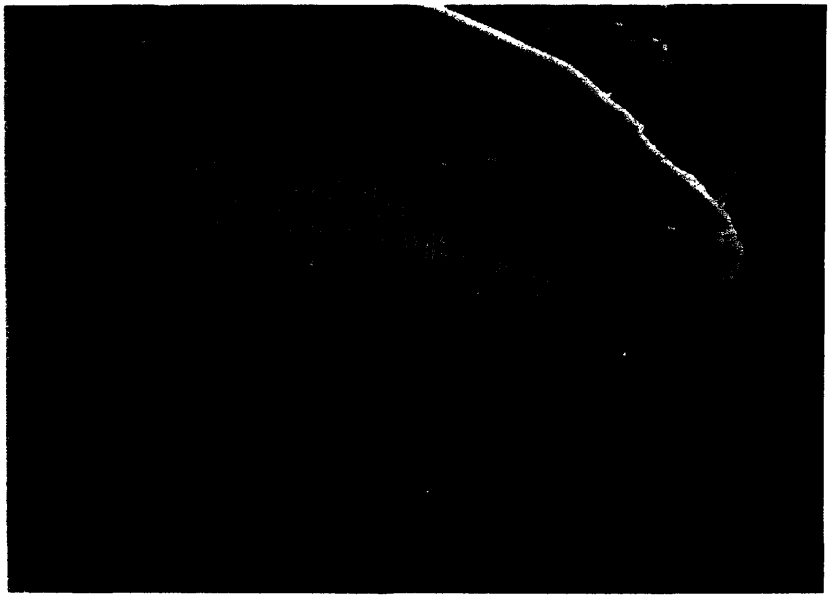

Fig. 33 A.R. Titanium Alloy, 800 feet/sec.


Fig. 34 Annealed Titanium Alloy, 800 feet/sec.

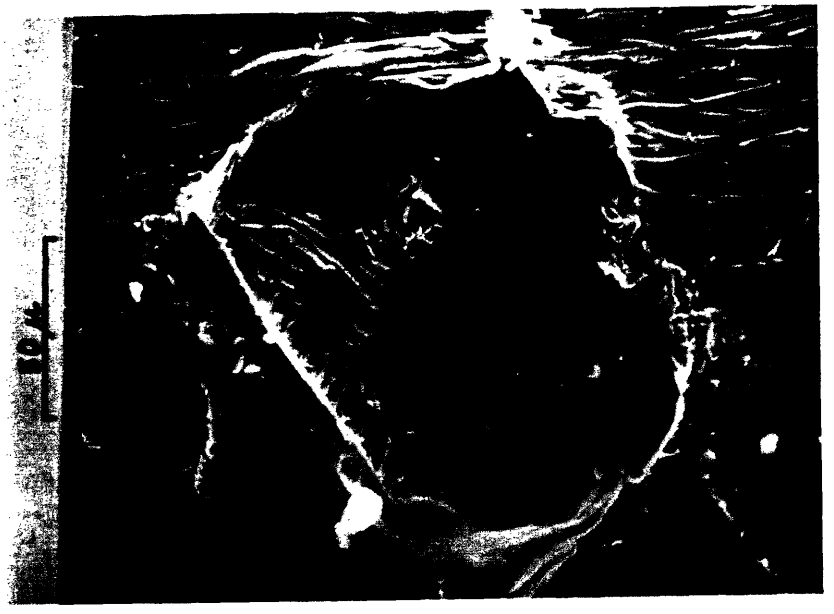


Fig. 35 CR 1020 Steel, 1000 Feet/sec.

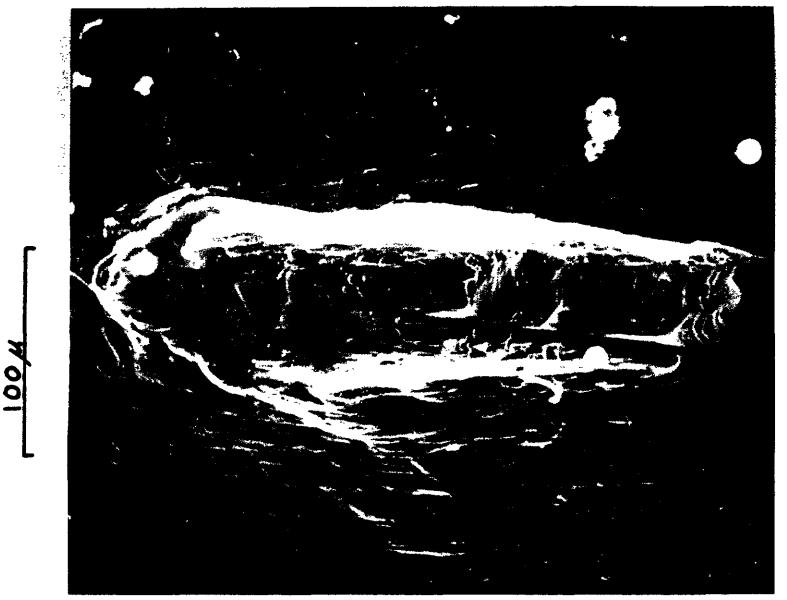


Fig. 36 Annealed 1020 Steel, 10[illegible]0 feet/sec.


Fig. 37 CR 1020 Steel, 10[illegible]0 Feet/sec.

Fig. 38 A.R. Modified 1010 Steel, 1000 feet/sec.


Fig. 39 Annealed Modified 1010 Steel, 1000 feet/sec.

Fig. 40 A.R. Titanium Alloy, 1000 feet/sec.

Discussion

The damage which occurred during the particle impingement tests relies on many factors. First among these is the strength of metals, which determines the degree of damage. A second contributing factor is material defects and variations in material compostion. Finally, the variations in speed may affect the damage to the specimens.

Tests over 1000 feet per second were not performed because of the limiting effect of the theoretical strength of metals. From atomic-bond theory:

$$\sigma_{theoretical} \cong \frac{E}{15}$$

and $$\sigma = E\varepsilon$$

$$\therefore \varepsilon_{theoretical} = .06$$

Now consider the case of a mass traveling at velocity V hitting a long rod. In time $\Delta t$ the end of the rod moves a distance $V\Delta t$.

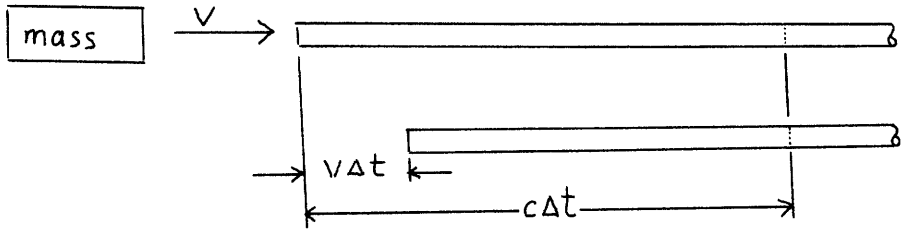


Fig. 41, Strain wave in a rod.

A stress wave travels in time $\Delta t$ a distance $c\Delta t$ where c is the speed of sound in the rod ( for steel, $c=1.66 \times 10^4$ ft/sec. ).

Since $$\varepsilon = \frac{\Delta \ell}{\ell} = \frac{V\Delta t}{c\,\Delta t} = \frac{V}{c}$$

then $$\frac{V}{c} \cong .06$$

Therefore, in order to remain within the theoretical strength, the maximum value of V must be less than approximately 1000 ft/sec. for steel. This assumes that the abrasive particles are rigid.

Our results with the small grained specimens are difficult to evaluate due to numerous voids throughout the specimens. These voids are clearly shown in Figures 13,15,17,18,19,25,26, 32, and 34. Material properties such as the compressive strength of the material may be drastically affected by such voids. The examination of the right side of Figure 26 with stereo viewers shows that apparently a section of the surface is depressed without showing any displaced metal elsewhere. This may be an indication that some of the voids were eliminated during the process.

An uncertainty was caused by particles other than the intended ones striking the surface of the specimens. Figures 13 and 14 both show chips which imbedded only slightly in the surface. No damage is observed as the chips appear to be just lying on the surface. Low velocity ( 100 ft/sec. ) is most likely a significant factor in the absence of damage. The chip in Figure 13 appears to have been freshly " machined " while the chip in Figure 14 looks as if it struck several things before finally lodging in the specimen.

At higher velocities, however, the damage caused by such chips may be quite severe as shown in Figures 26,29,32,and 34.

Since the particles lack the voids that are prevalent in the surface of the specimens, it is doubtful that they are of the same material. Furthermore, with the possible exception of Figure 26, the particles do not appear to be silicon carbide, a non-conductor which would appear white under the microscope. Most likely, the particles are chips from either the rotating arm or the sides of the test chamber. Figure 33 shows a large chip which imbedded in the surface. A similar chip hit the surface in Figure 32 but upon impact shattered into many smaller pieces. Figure 29 shows a dramatic example of fragmentation. Figures 30 and 31, which are both enlargements of Figure 29, show respectively 50-micron fragments and sub-micron fragments. Logically, all of the fragments in these pictures did not remain lodged and some would be free to strike the surface again causing more damage. It is unlikely that either the chips or the fragments of the chips would be stationary inside the test chamber; instead, they would be traveling at some unknown velocity. Since the specimen is moving at a known velocity, the impact speed would be the vector sum of the umknown velocity and the known velocity. Therefore our results are obscured by not knowing the true impact conditions.

Now that the uncontrollable aspects of the experiments have been examined, it is possible to discuss objectively the results of the controlled variations in the testing. As might be expected, increased impingement velocity generally resulted

in increased crater depth. Figures 10,11,12,and 15 all show shallow craters which were formed by particles traveling at 100 ft/sec. Slightly deeper craters were formed at 300 ft/sec. as shown in Figures 17 and 18, still deeper craters at 500 ft/sec. as shown in Figures 20, 22, and 25, and the deepest craters at 800 and 1000 ft/sec. as shown in Figures 27,28,35,38, and 39. This result is fairly conclusive as the 1020 steel acted in the same manner as the questionable materials in which voids were numerous.

The secondary damage which was mentioned before ( damage by fragmented particles and material ) also tends to increase with increasing test velocity. Only a general statement can be made since the true impinging velocity is not known. Figures 29,30, and 31 show an excellent example of secondary damage. Other examples are shown in Figures 26, 33, and 40.

So far, observations on the mechanisms of erosion have not been discussed in this paper. Finnie's model of micro-machining as mentioned in the introduction is possibly supported in four cases. It should be noted that his model was based on smaller impingement angles than 90°. However, due to the uncertainty in our testing, it is possible that this damage occurred from particles moving in unknown directions. Figure 34 shows a fragment of metal or silicon carbide which skimmed along the surface machining a groove until it lodged in the specimen. Figures 21 and 39 show a similar occurrence.

The foreign particle in Figure 39 was assumed to have been lodged after the erosion took place. In Figure 22, a larger particle could have skimmed from the lower left of the picture, machined a groove, and as it left, formed the large ridge. Figures 23 and 24 are enlargements of this damage.

The most prevalent form of damage, however, appears to be the pure shearing of the sides of the craters. Although the best examples of this are in Figures 38, 28, 20, and 10, shearing can also be seen in Figures 12,15, 18,19,22,25,26,27, 35,36,and 39. In Figure 12 it can be seen how cleanly the shearing took place. In the lower left corner, the voids were undisturbed during the shearing process.

Another very interesting occurrence is the appearance of fibrous material in the bottom of the craters. This looks very similar to the exposed surface of a ductile material after a tensile fracture. Figures 38,22,20, and 10 show this effect in decreasing clarity as do many of the other pictures listed above that show erosion in the shear mode.

Several other infrequent occurrences may also be noted. Figure 16 shows a small particle which imbedded in the surface of the specimen. Two fragments of the surface, equal to the size of the particle, have been almost broken loose. If the particle had had more energy, possible both the fragments and the particle would have left the surface and the resultant crater would have been similar to that in Figure 12. Another

interesting case is Figure 27 where the right crater is on the specimen's edge ( bright white lines ). The crater itself is cold worked and many voids have been formed. Also, no fluid-like flow appeared to take place in any of the cases, as had been previously reported by Sherman.[11]

Finally, no difference was observed in the erosion characteristics of the different materials. However, until the machanisms of erosion are more fully understood, observing the effects of impacts in different materials cannot accurately predict their respective erosion characteristics. For this reason, no conclusion is drawn as to the superiority of one metal over another.

## Conclusions

As a result of the 90° single particle impingement tests performed, the following conclusions may be drawn. The primary mechanism of this erosion appears to be pure shear. Uncertainties caused by secondary damage from both the specimen and the apparatus cloud the results of rotating arm erosion tests. Until the mechanisms of erosion are more fully understood, the analysis of materials should be done by more conventional erosion testing rather than by single particle impingement tests.

Bibliography


1. Tilly, G., "Erosion Caused by Airborne Particles," Wear, Vol.14, 1969,pp.63-79.

2. Smeltzer,C., Gulden,M., and Compton,W., "Mechanisms of Metal Removal by Impacting Dust Particles", ASME, Paper No. 69-WA/MET-8.

3. Bitter,J., "A Study of Erosion Phenomena, Parts I and II," Wear, Vol.6, 1963,pp.5-21.

4. Heymann, F., "Erosion by Liquids", Machine Design, December10, 1970, pp117-124.

5. Neilson, J., and Gilchrist,A., "An Experimental Investigation into Aspects of Erosion in Rocket Motor Tail Nozzles", Wear, Vol. 11, 1968,pp. 123-143.

6. Sheldon, G., and Finnie, I., "The Mechanism of Material Removal in the Erosive Cutting of Brittle Materials", Journal of Engineering for Industry, Nov. 1966, pp.393-400.

7. Finnie, Iain, "The Mechanism of Erosion of Ductile Metals", 1958, pp.527-532.

8. Finnie, Iain, "Erosion of Surfaces by Solid Particles", Wear, Vol.3, 1960, pp. 87-103.

9. Sheldon,G., and Finnie, I., "On the Ductile Behavior of Nominally Brittle Materials During Erosive Cutting", Journal of Engineering for Industry, Nov. 1966, pp.387-392.

10. Sheldon,G., "Similarities and Differences in the Erosion Behavior of Materials", ASME, Paper No. 69-WA/Met-7.

11. Sherman,Charles, "Wear of Metallic Surfaces by Particle Impingement", Unpublished Thesis,M.I.T., Jan., 1971.